A State-of-the-Art Review on Soft-Switching Techniques for DC–DC, DC–AC, AC–DC, and AC–AC Power Converters

Sadeq Ali Qasem Mohammed and Jin-Woo Jung, *Member, IEEE*

***Abstract*—Due to the continuously increasing demand on switched-mode power converters (i.e., dc–dc, dc–ac, ac–dc, and ac–ac) that can achieve high efficiency at high switching frequency, soft-switching techniques have received much attention in the area of power converter applications over recent years. This article provides a comprehensive review of the state-of-the-art soft-switching techniques used to achieve the zero-voltage switching and zero-current switching supplied by power switching devices. First, the auxiliary-circuit-based and nonauxiliary-circuit-based techniques that perform soft switching are systematically classified according to power converter. Next, soft-switching techniques for each power converter are comprehensively classified and reviewed in detail. Unlike the existing review papers that only categorize the soft-switching techniques used in dc choppers and inverters, this article offers further helpful categorization for all types of power converters. Further, it provides the merits, demerits, and suitable applications for each soft-switching technique. Finally, it suggests future research issues for soft-switching techniques in power converters.**

***Index Terms*—Auxiliary-circuit-based technique, nonauxiliary-circuit-based technique, switched-mode power converters, zero-current switching (ZCS), zero-voltage switching (ZVS).**

I. Introduction

POWER converters are extensively utilized in many applications such as consumer electronics, industrial electronics, electric vehicles (EVs), energy storage systems, and distributed generation systems to generate either a regulated dc or ac voltage source and manage the power flow by mainly controlling the switching actions of power semiconductor devices [1], [2]. In these power converters, hard-switching schemes have been extensively adopted owing to their uncomplicated structure and low cost topology in terms of the limited number of components needed to drive the switching devices [3], [4].

Unfortunately, these hard-switching schemes have well-known drawbacks when used in power converters such as high switching loss, low power density, high-frequency (HF) switching noise, low system efficiency, electromagnetic interference (EMI) emission, etc. [5], [6]. In applications where the hard-switching occurs, the balance between the demand for high switching frequencies and the acceptable system loss should be considered to meet the desired system efficiency [7], [8]. Since system efficiency is correlated with switching frequency, a low switching frequency is generally required to provide acceptably high efficiency. This can be achieved by lowering the cumulative amount of switching cycles for each transistor during the conversion process [9], [10]. However, this approach increases the size of other passive components (e.g., inductors and capacitors) and as a consequence the overall cost [9]. In addition, it produces high output ripples and high harmonic distortion, which then need to be filtered by larger output filters that lead to more increased costs, size, and weight to the overall system [10].

To overcome the aforementioned issues (e.g., switching loss, EMI, and switching stress) instigated by the hard switching, numerous soft switching techniques, which add a higher frequency resonant network to hard switching topologies, were reported in [4], [5]. Generally, soft-switching schemes, which perform zero-voltage switching (ZVS) and zero-current switching (ZCS), can be categorized into two different techniques: auxiliary-circuit-based techniques (i.e., hardware-based) [11]–[74] and nonauxiliary-circuit-based techniques (i.e., software-based) [75]–[112].

First, the auxiliary-circuit-based techniques can be classified according to the type of power converter used as follows: three techniques for dc–dc converters (i.e., quasi-resonant (QR)-based techniques [11]–[18], series/parallel/series-parallel resonant (SR/PR/SPR)-based techniques [19]–[24], multiple-resonant (MR)-based techniques [25]–[31], and resonant-transition (RT)-based techniques [32]–[37]), three techniques for the dc–ac converters (i.e., load-resonant (LR)-based techniques [38]–[45], RT-based techniques [46]–[50], and resonant-link (RL)-based techniques [51]–[57]), two techniques for the ac–dc converters [i.e., passive devices (PD)-based techniques [58]–[60] and active devices (AD)-based techniques [61]–[66]], and two techniques for the ac–ac converters [i.e., passive snubber (PS)-based techniques

Manuscript received September 28, 2020; revised November 12, 2020 and December 30, 2020; accepted February 5, 2021. Date of publication February 9, 2021; date of current version June 30, 2021. This work was supported by the Basic Science Research Program through the National Research Foundation of Korea funded by the Ministry of Education under Grant 2018R1D1A1B07046873. Paper no. TII-20-4510. *(Corresponding author: Jin-Woo Jung.)*

The authors are with the Division of Electronics and Electrical Engineering, Dongguk University, Seoul 04620, South Korea (e-mail: sadeqali9025@gmail.com; jinwjung@dongguk.edu).

Color versions of one or more figures in this article are available at https://doi.org/10.1109/TII.2021.3058218.

Digital Object Identifier 10.1109/TII.2021.3058218

[67]–[70] and active snubber (AS)-based techniques [71]–[74]. Despite the high efficiency offered by the auxiliary-circuit-based techniques stated above, their design not only increases the overall size and cost of a system, but it also increases the conduction loss as a consequence of the circulating currents in the auxiliary components. Further, the voltage/current ratings of switching devices increase as the peak values of the voltage/current in the resonant tank increase.

Second, the nonauxiliary-circuit-based techniques can be divided similarly according to the power electronic converters as follows: two techniques for dc–dc converters [i.e., single-phase-shift (SPS)-based technique [75]–[78] and dual-phase-shift (DPS)-based technique [79]–[83]], three techniques for the dc–ac converters [i.e., boundary current mode (BCM)-based technique [84], [85], constant hysteresis current mode (CHCM)-based technique [86], [87], and variable hysteresis current mode (VHCM)-based technique [88], [89]], three techniques for the ac–dc converters [i.e., phase-shift-modulation (PSM)-based technique [90]–[94], trapezoidal-modulation (TZM)-based technique [95]–[99], and triangular-modulation (TRM)-based technique [100]–[102]], and two techniques for the ac–ac converters (i.e., PSM-based techniques [103]–[107] and ac-link energy-based technique [108]–[112]). Unlike the soft-switching implemented by the auxiliary-circuit-based techniques, soft-switching by a phase-shift technique achieves reduced cost, high efficiency, and high reliability [77]–[78] because no unnecessary auxiliary components are present to make the overall system less reliable and costly. However, they are complex to control and the ZVS may fail under a light load due to the limited gain ratio, hence they are not recommended for low power applications [76]. Also, their soft-switching capability is limited because only a 50% duty ratio is allowed to ensure a suitable phase-angle between the two full bridges (FBs) of applications such as in dual-active-bridge (DAB) converters [79], [80]. Thus, to overcome this limitation, the DPS techniques have been adopted in a number of applications, in particular, DAB applications to extend the soft-switching range. Further, despite the long lifetime and high reliability of the switching devices achieved by all of the BCM, CHCM, VHCM, PSM, TZM, TRM, and ac-link energy-based techniques, they all require complex modulation and control structure [84]–[112].

This article presents a comprehensive review on the soft-switching techniques for switched-mode power converters (i.e., dc–dc, dc–ac, ac–dc, and ac–ac) adopted to achieve ZVS and ZCS in semiconductor switching devices [e.g., insulated-gate bipolar transistors (IGBTs), metal–oxide–semiconductor field-effect transistors (MOSFETs), etc.]. First, the auxiliary-circuit-based techniques and nonauxiliary-circuit-based techniques used to achieve the soft switching are systematically categorized according to the type of power converter. Next, the classification and deep discussion on both methods are provided while the soft-switching techniques for each power converter are addressed individually. Finally, it offers informative guidelines on the proper applications for each soft-switching technique along with their merits, demerits, and future research issues.

The rest of this article is organized as follows. Section II provides the classification of soft-switching techniques for power converters. Section III contains a deep discussion on auxiliary-circuit-based soft-switching techniques. Section IV thoroughly reviews nonauxiliary-circuit-based soft-switching techniques. Next, Section V details some future research issues for soft-switching techniques in power converters. Finally, Section VI concludes this article.

II. Classification of Auxiliary-Circuit-Based Techniques and Nonauxiliary-Circuit-Based Techniques to Achieve Soft Switching

For the past few decades, ongoing advancements in power electronic devices (e.g., MOSFETs, IGBTs, etc.) have not only led to the improvements in those power devices, but have also provided new concepts and techniques in controlling power converter topologies [10], [11].

Under hard switching, power switching devices have to intersect the voltage and current flowing through them during their ON/OFF states. This causes high stress and high switching loss on power converters, particularly for high switching frequency applications. Due to the issues that come with increasing the switching frequency, the switching frequency of typical converters is limited to a few tens of kHz, i.e., roughly 20∼50 kHz in the late of 1980s through the 1990s [14], [17]. However, advanced power switching devices and switching loss reduction achieved by ZVS and ZCS have helped to increase the switching frequency up to a couple of hundred kHz, i.e., 100∼500 kHz [9]. Generally, the concept of soft-switching can be applied by connecting a capacitor in parallel with the power switch to achieve the ZVS or by connecting an inductor in series with the power switch to achieve the ZCS. For ZVS, the main goal of resonant circuit is to manipulate the switch voltage waveform during the OFF-time to create ZVS turn-ON [5]–[7]. However, for ZCS, the switch current slowly rises from zero, then oscillates due to the resonance between inductor and capacitor resulting in ZVS turn-OFF.

Fig. 1 presents a systematic classification of main up-to-date techniques that are used to achieve soft switching in all power converters, while Fig. 2 shows the concept of ZVS and ZCS. As shown in Fig. 1, these techniques can be categorized into auxiliary-circuit-based techniques and nonauxiliary-circuit-based techniques. It is noted that each technique is classified based on the power converters [i.e., according to types (dc or ac) of input and output voltages applied to whole power converters] where the soft switching for switching devices is achieved by either integrating an auxiliary circuit with the power converters or by adopting a nonauxiliary-circuit-based technique. All techniques will be addressed in detail in Sections III and IV.

III. Auxiliary-Circuit-Based Soft-Switching Techniques

This section comprehensively discusses the auxiliary-circuit-based techniques that offer the soft switching for all types of power converters. As shown in Fig. 1, the switching techniques in dc–dc converters are first broken down into three groups (i.e., QR-based techniques [11]–[18], SR/PR/SPR-based techniques [19]–[24], MR-based techniques [25]–[31], and RT-based techniques [32]–[37]). Second, the switching techniques in dc–ac converters are subdivided into three groups (i.e., the LR-based

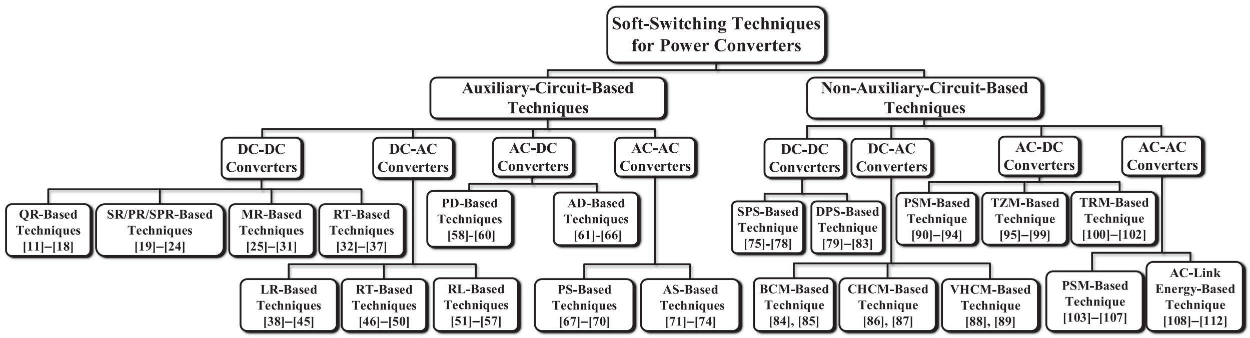

Fig. 1. Systematic classification of soft-switching techniques based on either auxiliary or nonauxiliary circuits for power converters.

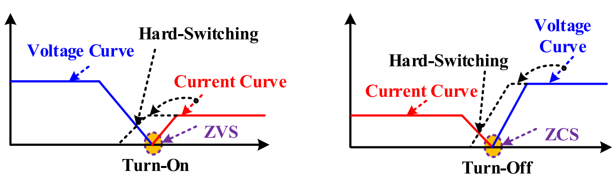

Fig. 2. Working concept of ZVS and ZCS [5], [6].

techniques [38]–[45], RT-based techniques [46]–[50], and RL-based techniques [51]–[57]). Third, the switching techniques in ac–dc converters are classified into two groups (i.e., PD-based techniques [58]–[60] and AD-based techniques [61]–[66]). Last, the switching techniques in ac–ac converters are sorted into two groups (i.e., PS-based techniques [67]–[70] and AS-based techniques [71]–[74]). Note that Section III-E is dedicated for some applications of the above basic soft-switching techniques. In this subsection, the basic soft-switching topologies are integrated with some standard converters to form a cascaded structure with a soft-swithcing purpose.

A. DC–DC Power Converters

This subsection details the QR-based techniques [11]–[18], SR/PR/SPR-based techniques [19]–[24], MR-based techniques [25]–[31], and RT-based techniques [32]–[37] adopted to perform the soft-switching (i.e., ZVS and ZCS) in dc–dc power converters.

1) Quasi-Resonant (QR)-Based Techniques: Even if the QR-based techniques [11]–[18] do not necessarily need extra components to work, they can be also constructed by adding some resonant elements to hard-switching dc–dc converters as depicted in Fig. 3(a)–(c). In the QR-based dc–dc converters, there are only two auxiliary elements which can be constructed by passive components either for medium power (1∼10 kW)/high power (>10 kW) applications [Fig. 3(a)] or for low power (<1 kW) applications [Fig. 3(b) and (c)], i.e., one capacitor (C_r) and one inductor (L_r) [12], [13], [15] or it can be formed by both active and passive components as shown in Fig. 3(c). The cyclic term in Fig. 3(b) indicates that there are two controllable switches instead of one active switch and one passive switch [13]. Thus, using the QR-based resonant cells, the ZVS and ZCS can be achieved for either the main switches or diodes, depending on how to connect the reactive components. Despite the low current stress on the main switches and simple design, the active switches are subjected to excessive voltage stress due to the high peak voltage in the resonant tank. Further, the interaction between the parasitic junction capacitance and the large resonant inductor creates a large noise from the switching oscillations [11]–[18].

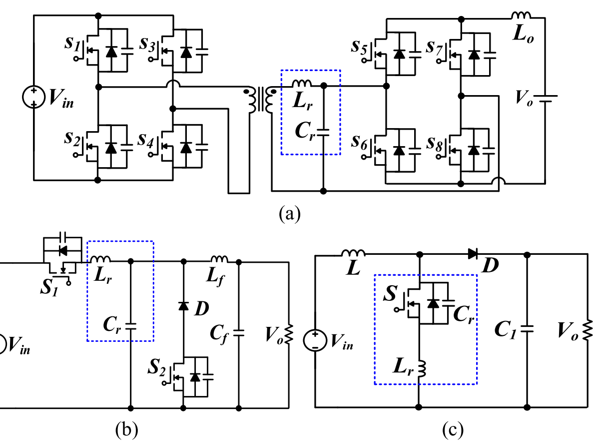

Fig. 3. QR-based techniques for dc–dc converters. (a) Bidirectional full-bridge dc–dc converter [12]. (b) Cyclic QR converter [13]. (c) ZVS QR dc–dc converter [15].

Thus, these particular techniques shown in Fig. 3(a)–(c) are suitable for dc–dc applications including small (<1 kW), medium (1∼10 kW), and high power (>10 kW) [6], [7], [17], [32], [95] applications, e.g., smart lighting, smartphones, EVs, etc. Their output power and switching frequency are used between 0.1∼10 and 35∼200 kHz, respectively, and these systems can achieve remarkable efficiencies of 85%∼98%. It should be noted that the power levels of presented switching-mode topologies are generally judged based on the number of power switches and the galvanic isolation (i.e., with or without transformer) to provide an electrical separation between input and output circuits [6], [73], [75]. Thus, as discussed in [6], for applications that demand high power along with safety, their power converters have to provide an electrical isolation with transformer [25], [62], [100]. Since these converters demand high-powered transformers, single-switch nonisolated converters (i.e., traditional buck, boost, buck–boost, etc.) [13], [15] and single-switch isolated converters (e.g., forward, flyback, etc.) [5] are not widely used for high-powered applications because a single-switch can be damaged due to high voltage

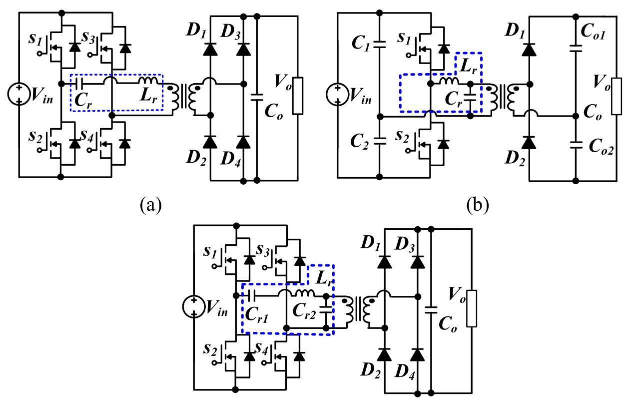

Fig. 4. SR/PR/SPR-based techniques for dc–dc converters. (a) SR converter [19], [20]. (b) PR converter [21], [22]. (c) SPR converter [23], [24].

stress caused by highly delivered power [6], [13], [15]. Thus, to increase the power level of these single-switch-based converters, advanced nonisolated converters (e.g., interleaved boost, interleaved buck–boost, etc.) [60], [86] or isolated converters (e.g., full-/half-bridge, push–pull, etc.) [5], [6], [35] with more than one controllable switch can be proper alternatives because they can be effectively functioned as current and voltage doubles [60], [64], [71], [86].

2) Series/Parallel/Series-Parallel Resonant (SR/PR/SPR)-Based Techniques: The SR/PR/SPR-based techniques [19]–[24] can be identified according to the connection of inductor and capacitor at resonant tank, i.e., series [19], [20], parallel [21], [22], or series–parallel [23], [24]. For the SR and PR converters, the inductor and capacitor is connected in series and parallel with an auxiliary resonant tank, respectively, as shown in Fig. 4(a) and (b). However, in the SPR converter [Fig. 4(c)], one capacitor at resonant tank is in series connection with the inductor (L_r) and the other one is connected in parallel with the load. Despite the soft-switching achieved by these methods, the converter components suffer from voltage and current stress due to the location of the resonant tanks in power flow path. This in return limits their applications in high power levels. Thus, such topologies are suitable for constant load applications with output power and switching frequency ranging between 0.2$\sim$35 and 20$\sim$90 kHz, respectively, with maximum efficiency of 97%.

3) Multi-Resonant (MR)-Based Techniques: The MR-based techniques are an extended form of QR-based techniques [25]–[31]. These techniques are constructed from multiple reactive elements (L_r, C_r), i.e., the series configuration of capacitors and inductors as shown in Fig. 5(a), or parallel configuration of capacitors and inductors as shown by the blue dotted box in Fig. 5(b) and (c).

As shown in Fig. 5, the reactive cell consists of two resonant inductors and two resonant capacitors. In [25]–[31], two connection modes are adopted to achieve the ZVS and ZCS that can be concurrently offered for the main switches and diodes. Consequently, the MR-based techniques are recognized as double-ZVS/ZCS converters. Despite the high conduction loss created by circulating currents, there are less switching loss and noise reduction (i.e., all switching devices operate under ZVS) with the MR-based converters. Unlike the QR-based techniques [25], [26], the MR-based techniques have wider control dynamics, wide range of ZVS, and moderate voltage/current stress. Thus, they are preferred for medium power level dc–dc applications such as HF-link on-board chargers (OBCs) for EVs. Additionally, notched filters are used with MR converters [Fig. 5(a)], dual-transformer MR converters [Fig. 5(b)], and MR converters [Fig. 5(c)] with the output power range between 0.4$\sim$3 kW and the switching frequency between 50$\sim$145 kHz, and the high efficiencies of 90%$\sim$97%.

4) Resonant Transition (RT)-Based Techniques: Fig. 6 shows an RT cell built from a collection of auxiliary elements (i.e., some auxiliary switches and auxiliary resonant tanks shown inside the blue dotted box).

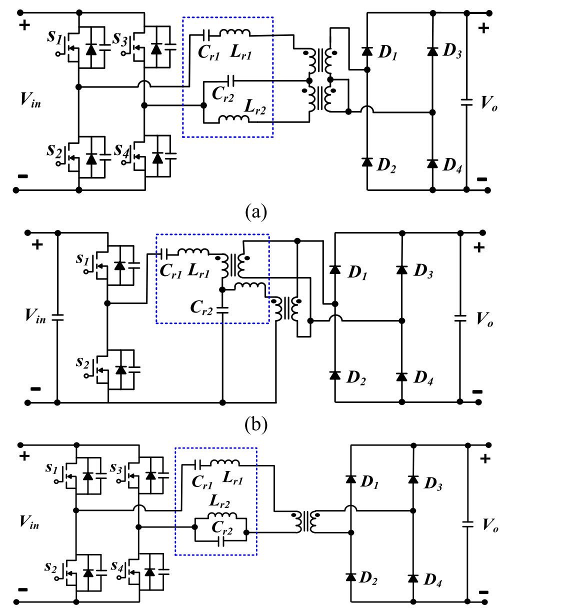

Fig. 5. MR-based techniques for dc–dc converters. (a) Notch filter MR converter [25]. (b) Dual-transformer MR converter [26]. (c) MR converter [27].

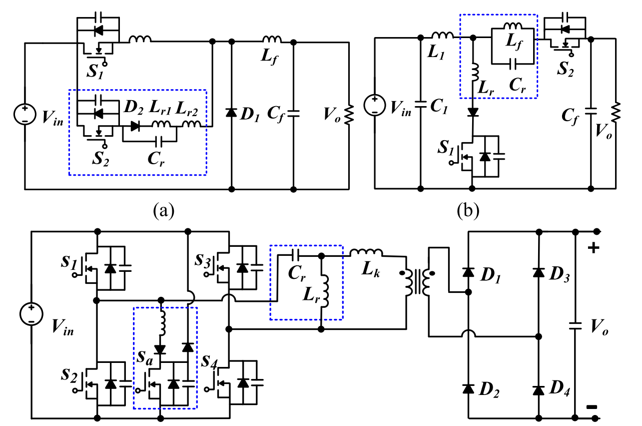

Fig. 6. RT-based techniques for dc–dc converters. (a) ZVT–ZCT buck converter [32]. (b) Resonant boost converter [34]. (c) Full-bridge CLL resonant converter [35].

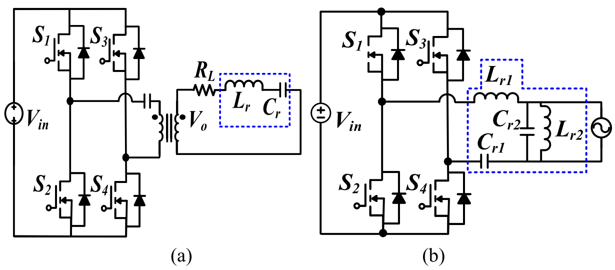

Fig. 7. Load resonant (LR)-based techniques for dc–ac converters. (a) Series-resonant converter [39]. (b) Parallel-resonant converter [41].

As documented in [32]–[37], the auxiliary cell is designed to offer zero current transition (ZCT) or zero voltage transition (ZVT) operation that turns-OFF the main switch when the current passing through it is zero and turns-ON the switch when the applied voltage across it is zero, respectively. Though these techniques improve the efficiency to some extent, they have several demerits, e.g., high circulating current, high peak current/voltage stress, and limited voltage conversion range [32]–[37]. These specific techniques are good candidates for various dc–dc applications, e.g., small/medium/high power level such as buck/boost/full-bridge converters in Fig. 6(a)–(c), respectively. Their output power and switching frequency ranges are between 0.1∼50 and 50∼400 kHz, respectively. In addition, their efficiency can reach up to 98%.

B. DC–AC Power Converters

This subsection addresses the LR-based techniques [38]–[45], RT-based techniques [46]–[50], and RL-based techniques [51]–[57] used to realize soft-switching (i.e., ZVS and ZCS) for dc–ac power converters.

1) Load Resonant (LR)-Based Techniques: For the past decades, pulsewidth modulation dc–ac converters have been used as the main choice for various applications such as in uninterruptible power supply systems, induction heating systems, and ac motor drives due to their good points, e.g., excellent and rugged control performance, and circuit simplicity [38]–[41].

Conversely, the high switching loss limits the operation of the power switches to a few kHz in cases where the power rating is tens of kW. Thus, LR-based inverter topologies are among promising solutions to handle the above problems. For instance, simplified topologies [42]–[43] with reduced auxiliary power switching counts were developed to achieve a soft switching for induction heating applications. As shown in Fig. 7, the resonant cell for LR-based techniques can be constructed by utilizing some passive elements such as L_r and C_r (shown inside the blue dotted box) or by adopting some additional auxiliary circuits that include some diodes or switches [38]–[45]. These components are connected to the load side in series [Fig. 7(a)], parallel [Fig. 7(b)], or both. These techniques can offer a high efficiency of up to 97%. Also, their corresponding power and switching frequency are within the range of 0.6∼5.5 and 8∼160 kHz, respectively.

2) Resonant Transition (RT)-Based Techniques: In the RT-based techniques depicted in Fig. 8, a resonant network with some auxiliary switches is integrated with the inverter bridge, thus creating the ZVT or ZCT for the main switching devices [46]–[50]. As shown in Fig. 8(a), the number of controllable auxiliary switches added to most soft-switching inverters is fewer than six, whereas there exist a few soft-switching inverters using six controllable auxiliary switches [Fig. 8(b)]. Unlike the latter, the former approach achieves low cost, reduced size, and better soft-switching performance [46]–[50]. Thus, connecting the resonant components in parallel or series with the main power switches creates HF resonance, which in return offers ZVT or ZCT. The above-stated advantages improve the system's efficiency up to 98% and make them suitable for power dc–ac converters with output power and switching frequency ranges of 0.5∼50 and 10∼400 kHz, respectively.

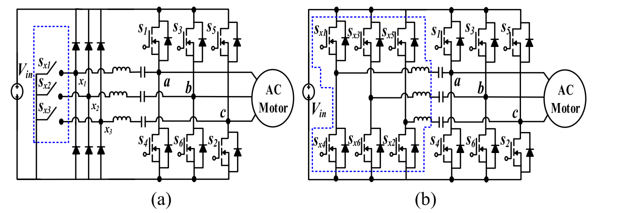

Fig. 8. Resonant transition (RT)-based techniques for dc–ac converters. (a) Three-phase ZCT inverter with three controllable auxiliary switches inverter [48]. (b) Three-phase ZCT inverter with six controllable auxiliary switches [48].

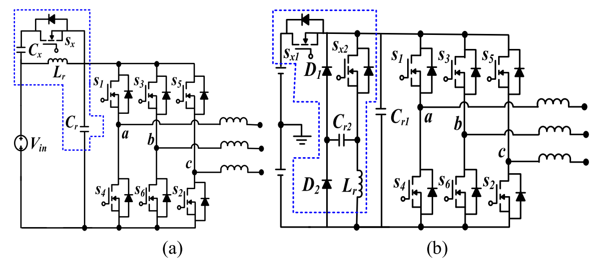

Fig. 9. Resonant link (RL)-based techniques for dc–ac converters. (a) Current-fed parallel dc link inverter [51]. (b) Voltage-fed quasi-parallel resonant dc link inverter [53].

3) Resonant Link (RL)-Based Techniques: Fig. 9 illustrates the RL-based circuit placed between the rectified voltage and the dc–ac bridge, which is built from some passive components and some active components (link diodes and controlled switches) [51]–[57], as shown inside the blue dotted box.

Exchanging energy between the resonant components produces some oscillations in the input bus, which contributes to the improvement of system efficiency by achieving soft switching for switching devices. The efficiency provided via these techniques can reach up to 98%. These techniques can be utilized for any form of current-fed/voltage-fed dc–ac resonant converters, as shown in Fig. 9(a) and (b), with output power and switching frequency in the range of 0.5∼50 and 10∼400 kHz, respectively.

C. AC–DC Power Converters

The PD-based techniques [58]–[60] and AD-based techniques [61]–[66] for ac–dc power converters are addressed in detail in this subsection.

1) Passive-Devices (PD)-Based Techniques: The PD-based techniques [58]–[60] utilize only passive elements (e.g.,

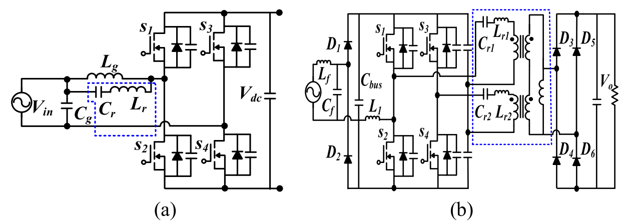

Fig. 10. Passive-devices (PD)-based techniques for ac–dc converters. (a) Series PD resonant rectifier [58]. (b) Parallel PD resonant rectifier [59].

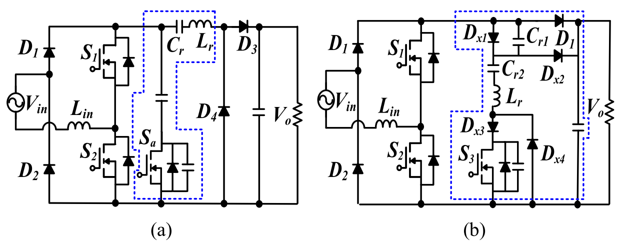

Fig. 11. Active-devices (AD)-based techniques for ac–dc converters [64], [66]. (a) First structure. (b) Second structure.

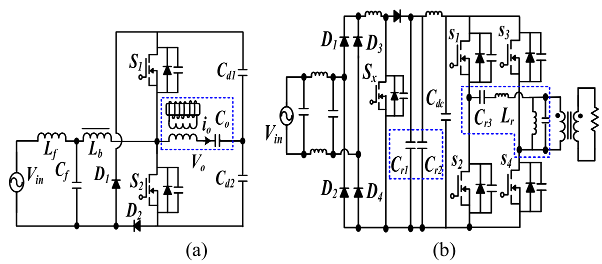

Fig. 12. Passive snubber (PS)-based techniques for ac–ac converters. (a) First structure [67]. (b) Second structure [70].

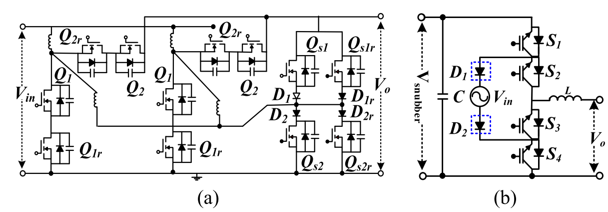

Fig. 13. Active snubber (AS)-based techniques for ac–ac converters. (a) First structure [72]. (b) Second structure [74].

inductors and capacitors) to achieve soft switching for ac–dc converters, which can be connected in series or parallel, respectively, as shown in Fig. 10(a) and (b). Also, the series and parallel resonant tanks can be integrated to build a series–parallel connection. Thus, they can offer high efficiency, particularly, in high power applications. However, they have some limitations as they can only achieve soft switching for the main switches.

In Fig. 10, ZCS is attained during a switching interval that heavily depends on the resonant network (indicated by the blue dotted box). In this circuit, the resonant components can create some delay, but help to obtain soft commutation in the main switches (S_1 and S_2) as well as in the diodes. These techniques are acceptable for certain applications, e.g., the series and parallel PD resonant rectifiers shown in Fig. 10(a) and (b), respectively. The power and switching frequency ranges of the above applications can be 0.1$\sim$5 and 20$\sim$370 kHz, respectively, and their efficiency can reach up to 95%.

2) Active-Devices (AD)-Based Techniques: The AD-based techniques [61]–[66] adopt additional active switches and resonant elements to remarkably improve the efficiency of the overall system by overcoming the hard-switching intersections during the switches ON/OFF states. They have different structures [i.e., a single resonant cell with either series or parallel connection of L_r and C_r (Fig. 11(a)] and dual resonant cells with either series or parallel connection of L_r, C_{r1}, and C_{r2} [Fig. 11(b)] depending on the desired efficiency needed for a given application. In Fig. 11(a) and (b), the active switches S_a and S_3 are added to the ac–dc converters as auxiliary components to help in achieving the soft-switching during the OFF-state of S_1 and S_2. Nevertheless, some losses are partially exposed in the auxiliary circuit and cannot be eliminated.

Thus, this method is preferred for resonant rectifiers that have power, switching frequency, and efficiency ranges between 1$\sim$3 kW, 80$\sim$220 kHz, and 90$\sim$99%, respectively, because in high power applications they suffer from severe conduction loss. Further, in [62], a resonant bridgeless ac–dc rectifier with high switching frequency offers ZVS for the controlled switches and ZCS for the blocking diodes while inherently provides a power factor correction (PFC) capability. Meanwhile, a newly developed ac–dc [63] attributed with soft switching in both the ac side and dc side is presented by mananging the commutation of the ac side power switches along with a series inductor.

D. AC–AC Power Converters

This subsection reviews the PS-based techniques [67]–[70] and AS-based techniques [71]–[74] used to offer soft switching for ac–ac power converters.

1) Passive Snubber (PS)-Based Techniques: Fig. 12(a) displays one of the common PS (or lossless snubber) circuits [67]–[70] adopted for HF ac–ac converters that consists of a boost PFC circuit, input inductor (L_f), bridgeless rectifying diodes (D_1 and D$_2$), active switches (S_1 and S_2), and dc-link capacitors (C_{d1} and C_{d2}). In this configuration, the PS employs a resonant tank before the load is constructed by the transformer leakage inductance along with C_o.

Another structure can be formed by using different configurations of C_{r1} and C_{r2} on the ac link, as shown in Fig. 12(b). Thus, these techniques achieved an improved overall system efficiency that can reach up to 95%. Therefore, they are preferred in applications such as lossless snubber resonant ac–ac converters, which have power and switching frequency ranges of 0.2$\sim$3 kW and 12$\sim$100 kHz, respectively.

2) Active Snubber (AS)-Based Techniques: As depicted in Fig. 13(a), an AS circuit [71]–[74] is employed to realize soft switching.

As compared to the PS-based technique in Fig. 10, this circuit consists of some active switching devices (Q_{s1}, Q_{s1r}, Q_{s2}, and Q_{s2r}) along with some diodes ($D_1$$\sim$$D_4$) to form the AS block. Also, another low cost AS circuit can be built as shown in Fig. 13(b). The hard switching of the main switches is overcome

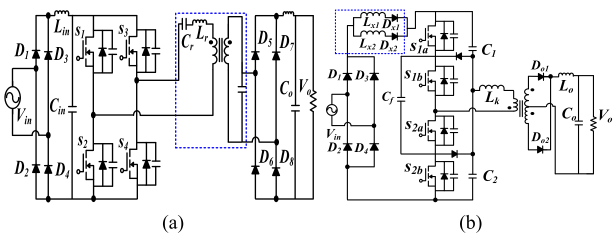

Fig. 14. Cascaded structure for soft-switching ac–dc converters with PD-based dc–dc techniques [61], [62]. (a) First structure. (b) Second structure.

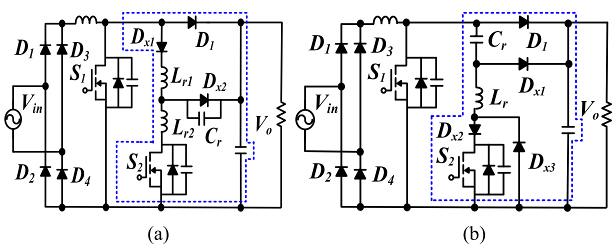

Fig. 15. Cascaded structure for soft-switching ac–dc converters with AD-based dc–dc techniques [65], [66]. (a) First structure. (b) Second structure.

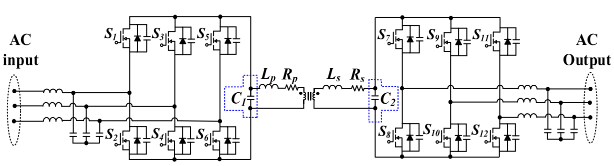

Fig. 16. Cascaded structure for soft-switching ac–ac converters with soft-switching ac–dc converter followed by dc–ac converter [69].

with this AS block by providing them with soft switching, i.e., it can achieve not only ZVS, but also ZCS for the entire operation of the switching devices. Soft switching is achieved by extracting the energy stored in the drain-source capacitors of the main switches and then delivering it to the high-voltage side of the ac–ac converter. Thus, these particular techniques can offer an efficiency of 95%, making it a good candidate for certain applications, e.g., AS resonant ac–ac converters in the ranges of 0.5$\sim$50 kW and 5$\sim$150 kHz.

E. Some Applications of Basic Soft-Switching Topologies

This subsection provides some applications of the above basic soft-switching topologies such as PFC ac–dc, back-to-back ac–dc–ac conveters, etc. as shown in Figs. 14 –16, respectively.

As depicted in Figs. 14 and 15, some of basic soft-switching-based dc–dc topologies that are built from either auxiliary PD (Fig. 14) or AD (Fig. 15) are integrated with ac–dc converters for soft-switching and PFC purposes [59], [60], [65], [66].

Another cascaded structure for ac–ac converters [69] is contructed from soft-switching ac–dc converter followed by dc–ac converter that includes two lossless capacitors (C_1 and C_2) to attain soft switching for all power switching devices [64] as viewed in Fig. 16. In this topology, the C_1 and C_2 function as a

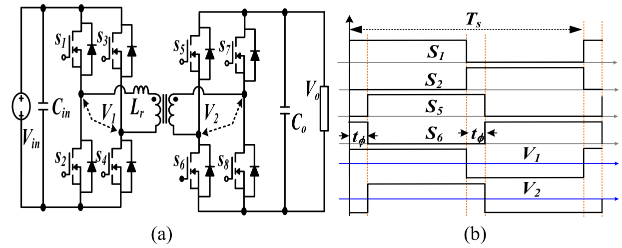

Fig. 17. Single-phase-shift (SPS)-based technique for dc–dc converters. (a) DAB topology [76]. (b) Single-phase gate-pulse pattern [76], [77].

PS to overcome the voltage spikes caused by the leakage inductances of HF-transformer during the OFF-time of input/output switches [64]. The charging modes take place when the link C_1 is connected to an input phase while discharging modes occur when the link C_2 is connected to an output phase. However, the resonant modes are created during the OFF-time of all switches.

IV. Nonauxiliary-Circuit-Based Soft-Switching Techniques

This section presents the classification and discussion of nonauxiliary-circuit-based techniques to realize soft switching in all power converters. First, the switching techniques in dc–dc converters are classified into two groups, namely, SPS-based technique [75]–[78] and DPS-based technique [79]–[83]. Next, the switching techniques in dc–ac converters are sorted as three groups (i.e., BCM-based technique [84], [85], CHCM-based technique [86], [87], and VHCM-based technique [88], [89]). Then, the switching techniques in ac–dc converters are broken down into three groups: PSM-based technique [90]–[94], TZM-based technique [95]–[99], and TRM-based technique [100]–[102]. Last, the switching techniques in ac–ac converters are subdivided into two groups, i.e., PSM-based technique [103]–[107] and ac-link energy-based technique [108]–[112].

A. DC–DC Converters

This subsection presents the SPS-based technique [75]–[78] and DPS-based technique [79]–[83] used to realize soft switching in dc–dc power converters.

1) Single-Phase-Shift (SPS)-Based Technique: As shown in Fig. 17, the SPS-based technique [75]–[78] is achieved by creating a phase-shift between the two bridges of the dc–dc converter (i.e., a phase-shift angle (t_ϕ) between S_1/S_2 and S_5/S_6) with an effective duty cycle of 50%.

As shown in Fig. 17(b), the angle (t_ϕ) controls the zero voltage period of the voltage applied between the two bridges, so ZVS/ZCS can be inherently accomplished. For instance, it is mainly of interest to adopt the phase-shift control technique for bidirectional DAB converters for many kinds of high power applications because of its inherent soft switching, high power density capability, and high efficiency. However, ZVS is not achieved under light loads due to limitations of the gain ratio. To overcome this problem, the DPS approach [75]–[78] can be adopted to extend the gain ratio as the duty can vary compared to the PSM-based methods. Thus, they are an effective choice for certain applications, i.e., SPS dc–dc converters for ON/OFF-board

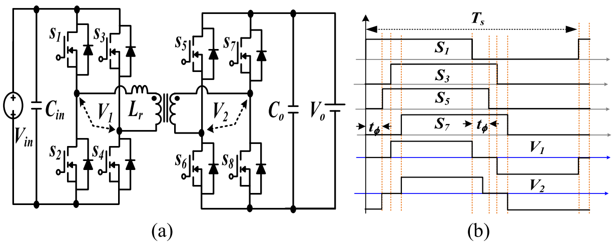

Fig. 18. Dual-phase-shift (DPS)-based technique for dc–dc converters. (a) DAB topology [80]. (b) Dual-phase gate-pulse pattern [82], [83].

battery chargers that have power/switching frequency ranges between 0.5∼80 kW and 5∼20 kHz, respectively. They can also achieve an excellent efficiency of up to 95%.

2) Dual-Phase-Shift (DPS)-Based Technique: The DPS-based technique [79]–[83] is developed to extend the soft-switching range, which consists of two phase-shifts: a phase-shift between the primary and secondary sides of the isolated transformer and a phase-shift between the gate signals of the switching devices. Note that Fig. 18(a) is a bidirectional full-bridge dc–dc converter similar to Fig. 17(a), except that it uses an alternative phase-shift. In this figure, the phase-shift between the two isolated sides (i.e., the primary and secondary sides) shown in Fig. 18(b) does not only control the power flow between the dc source side and the load side, but also helps in achieving both ZVS and ZCS in all switching devices. To this end, this technique is suitable for applications where high power quality is required, e.g., isolated bidirectional DAB dc–dc converters. Their corresponding power and switching frequency are within the ranges of 0.3∼15 kW and 20∼50 kHz, respectively.

B. DC–AC Converters

This subsection takes a deep look at the BCM-based technique [84], [85], CHCM-based technique [86], [87], and VHCM-based technique [88], [89] used to accomplish soft switching in dc–ac power converters. With these particular techniques, soft switching is achieved via controlling the inductor current, so current control (CC)-based techniques, e.g., BCM-based technique, CHCM-based technique, and VHCM-based technique are demanded to control the inductor current to attain ZVS for the power switches.

1) Boundary Current Mode (BCM)-Based Technique: First, the BCM [84], [85] in Fig. 19(a) is distinguished by its fixed reverse current (i.e., ΔI), where the peak-currents I_{p+} and I_{p-} can be obtained as follows:

$$\begin{cases} I_{p+} = 2I_{o,\text{peak}} \sin \omega t + \Delta I \\ I_{p-} = -\Delta I \end{cases} \tag{1}$$

where ω $(= 2\pi f)$ is the angular frequency and f is the switching frequency. Then, the summation of the peak currents can be rewritten as

$$I_{p+} - I_{p-} = 2(I_{o,\text{peak}} \sin \omega t + \Delta I). \tag{2}$$

Note that this technique achieves soft switching by harvesting the use of body capacitors of the main power switching devices as well as the output inductor without an auxiliary circuit.

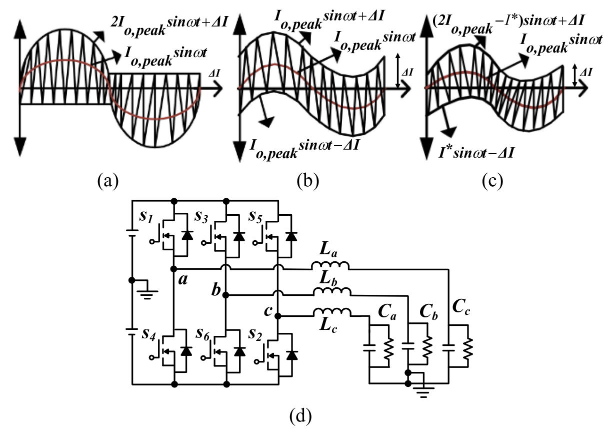

Fig. 19. Soft-switching for dc–ac converters. (a) BCM [79]. (b) CHCM [86]. (c) VHCM [89]. (d) DC–ac topology employing BCM/CHCM/VHCM [87].

2) Constant Hysteresis Current Mode (CHCM)-Based Technique: Unlike the BCM, the CHCM [86], [87] in Fig. 19(b) is characterized by its constant hysteresis band. In this technique, the peak currents I_{p+} and I_{p-} can be given as

$$\begin{cases} I_{p+} = I_{o,\text{peak}} \sin \omega t + \Delta I \\ I_{p-} = I_{o,\text{peak}} \sin \omega t - \Delta I \end{cases} \tag{3}$$

and the peak currents of this technique can be given by

$$I_{p+} - I_{p-} = 2\Delta I \tag{4}$$

where the reverse current (i.e., ΔI) is achieved in the same way as the BCM except that the reverse current is twice that of the BCM-based method.

3) Variable Hysteresis Current Mode (VHCM)-Based Technique: Unlike the BCM and CHCM, the VHCM [88], [89] in Fig. 19(c) has a variable current band associated with its variable reverse current.

As shown in Fig. 16(c), the variable peak currents (i.e., I_{p+} and I_{p-}) can be represented as

$$\begin{cases} I_{p+} = (2I_{o,\text{peak}} - I^*) \sin \omega t + \Delta I \\ I_{p-} = -I^* \sin \omega t - \Delta I. \end{cases} \tag{5}$$

$$I_{p+} - I_{p-} = 2[(I_{o,\text{peak}} - I^*) \sin \omega t + \Delta I]. \tag{6}$$

The above-discussed techniques can be used for numerous power applications (e.g., full-/half-bridge inverter topologies). To this point, among these techniques, the BCM can achieve better soft switching due to the fixed reversed current (1). Their output power and switching frequency ranges are between 0.2∼0.8 kW and 20∼240 kHz, respectively. Additionally, their efficiency can reach up to 98%.

C. AC–DC Converters

This subsection comprehensively details the PSM-based technique [90]–[94], TZM-based technique [95]–[99], and TRM-based technique [100]–[102] used to perform soft-switching in ac–dc power converters.

1) Phase-Shift-Modulation (PSM)-Based Techniques: The PSM-based technique [90]–[94] on the left-hand side of Fig. 20(b) is widely used for many isolated converters, e.g.,

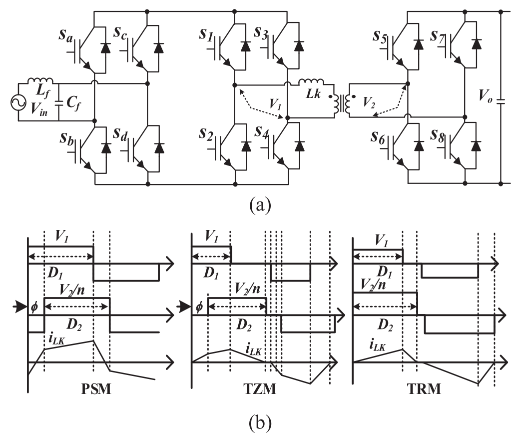

Fig. 20. PSM/TZM/TRM-based soft switching for ac–dc DAB converters. (a) DAB [92]. (b) PSM/TZM/TRM switching methods [92], [93].

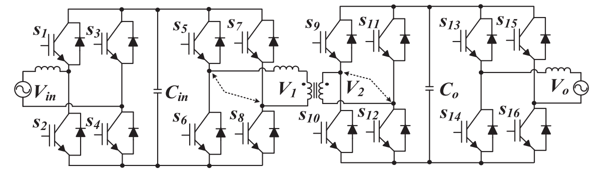

Fig. 21. PSM-based soft-switching for ac–ac converters [106].

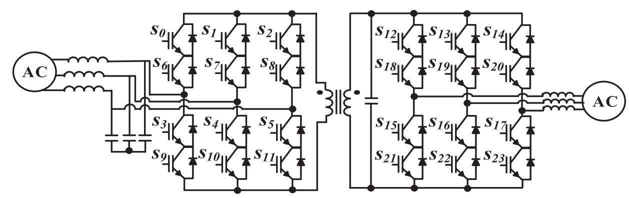

Fig. 22. AC-link energy-based soft switching for ac–ac converters [108].

the bidirectional DAB ac–dc converters shown in Fig. 20(a), because it regulates the forward/backward current flow between the primary-side and secondary-side and offers soft-switching for main switching devices. In Fig. 20(b), the top, middle, and bottom waveforms belong to the primary and secondary-side voltages and the leakage current (i.e., V_1, V_2/n, and i_{LK}, respectively) of the transformer in the DAB converters.

Also, this technique is simple and easy to control. However, it has limited soft switching because only a 50% duty ratio (i.e., the duty cycles for the applied voltages V_1 and V_2 are identical ($D_1 = D_2$)) is allowed to create the phase angle between the two FBs of DAB converters. To satify the above condition (i.e., $D_1 = D_2$), V_1 should be equal to V_2/n ($V_1 = V_2/n$) where n is the transformer turns ratio. This means a large reactive current flow and poor efficiency at light loads. Meanwhile, due to its stated merits, it can be effectively utilized for applications such as on-board battery chargers in EVs and telecom power supplies [90]–[94]. Finally, this method has the power range, switching frequency, and efficiency of 0.5∼5 kW, 20∼50 kHz, 86∼90%, respectively.

2) Trapezoidal-Modulation (TZM)-Based Technique: The TZM-based technique [95]–[99] in the middle of Fig. 20(b) overcomes the problem of a PSM-based technique due to its advantages of having three control options: two duty ratios and phase-shift. Moreover, it has a high power transfer capability because the duty cycle is not limited to 50%. The duty ratio D_2 of the applied voltage V_2 is determined as $D_2 = (D_1 \times V_1)/(V_2/n)$ where D_1 can be set to a value less than 50%. However, the applicability of this method is limited due to the condition that the transformer should have the turns ratio (i.e., $V_1 \approx V_2/n$) for given input and output voltages V_1 and V_2.

3) Triangular-Modulation (TRM)-Based Technique: The TRM-based technique [100]–[102] on the right-hand side of Fig. 20(b) is a special case of a TZM-based technique. Unlike the TZM-based technique, this technique is generally used in the condition that the voltages V_1 and V_2/n are significantly different [100]–[102] and D_2 can be easily calculated similar to that of the TZM-based method. However, it has an ineffective converter utilization because the transformer turns ratio should satisfy the condition (i.e., $V_1 < V_2/n$) for the whole range of given input and output voltages. Due to the low power transfer capability of this technique, it is suitable for low power ac–dc applications such as single-stage PFC-based rectifiers with the power range, switching frequency, and efficiency of 50∼250 W, 20∼50 kHz, and 85∼90%, respectively.

D. AC–AC Converters

This subsection discusses the PSM-based technique [103]–[107] and ac-link energy-based technique [108]–[112] that provide soft switching in ac–ac power converters.

1) Phase-Shift-Modulation (PSM)-Based Technique: Fig. 21 shows the PSM-based technique [103]–[107] used for DAB ac–ac converters that is constructed with an HF transformer and two-active H-bridges, i.e., the primary/secondary full-bridge.

For this specific converter, the source V_{in} is a low-frequency ac that is first converted to an HF V_1. Note that the phase-shift between V_1 and V_2 in Fig. 18 controls the delivered power from V_1 to the dc-link on the secondary-side of transformer [106]. Then, the HF V_1 is converted back to a low-frequency V_o by the right H-bridge of the secondary-side that acts as an inverter to control the delivered power to the low frequency source V_o. Thus, this converter is a type of back-to-back voltage source converter which is adopted to provide galvanic isolation, energy storage in its leakage winding, voltage regulation, and soft switching via the nonzero leakage. Then, they are suitable for DAB-based ac–ac applications with the power and switching frequency ranges of 0.5∼15 kW and 25∼100 kHz, respectively. Also, their efficiency can reach up to 98%.

2) AC-Link Energy-Based Technique: Fig. 22 shows the ac-link energy-based technique [108]–[112] for ac–ac converters. In these articles, ZVS/ZCS can be achieved by controlling the frequency of charging and discharging currents at the ac-link.

The soft commutation results in a long lifetime and high reliability for the switching devices. Thus, it is useful for applications such as variable-speed ac drives, direct distributed systems in wind-turbine generators, among others. Their power level and switching frequency are in the range of 0.2∼1.6 kW and 20∼120 kHz, respectively. Also, they can achieve high efficiencies of 93∼95%. Table I summarizes the soft-switching

TABLE I
SUMMARY OF SOFT-SWITCHING TECHNIQUES FOR POWER CONVERTERS

Converters		Techniques	Switching Frequency [kHz]	Maximum Efficiency [%]	Power Level [kW]	Applications	Remarks
DC-DC	①	Quasi-Resonant [11]–[18]	35 ~ 200	98	0.1 ~ 10	Electric Vehicles	■ Two reactive elements are added
		Series/Parallel/ Series-parallel Resonant [19]–[24]	20~ 90	97%	0.2 ~ 35	Constant load applications	■ Inductor and capacitor are connected in series, parallel or both at resonant tank
		Multiple-Resonant [25]–[31]	50 ~ 145	97	0.4 ~ 3	Power supplies for servers, battery charger for EVs	■ Multiple reactive elements are needed
		Resonant-Transition [32]–[37]	50 ~ 400	98	0.1 ~ 5	Power application system with high-voltage DC-link	■ Constructed by adding active/reactive components
	②	Single-Phase-Shift [75]–[78]	5 ~ 20	95	0.5 ~ 80	Modern transportation systems	■ 50% duty ratio used
		Dual-Phase-Shift [79]–[83]	20 ~ 50	97	0.3 ~ 15	DAB applications	■ Extended duty cycle
DC-AC	①	load resonant [38]–[45]	8 ~ 160	97	0.6 ~ 6	UPS systems, motor drives	■ Resonant network is connected to the load side in series/parallel connection
		Resonant transition [46]–[50]	10 ~ 400	98	0.5 ~ 50		■ Constructed by adding active/reactive components
		Resonant Link [51]–[57]	5 ~ 400	98	0.4 ~ 60		■ Resonant network is connected to the DC-link
	②	Boundary Current Mode [84], [85]	20 ~ 240	97	0.2 ~ 0.8	CM-based rectifiers	■ Fixed reverse current
		Constant Hysteresis Current Mode [86], [87]					■ Constant hysteresis band
		Variable Hysteresis Current Mode [88], [89]					■ Variable current band
AC-DC	①	Passive Devices [58]–[60]	20 ~ 370	95	0.1 ~ 5	Light emitting diodes rectifiers	■ Require passive components
		Active Devices [61]–[66]	80 ~ 220	99	1 ~ 3	Single power conversion rectifiers	■ Require active components
	②	Phase-Shift-Modulation [90]–[94]	20 ~ 50	90	0.5 ~ 5	Single/two-stage DCM rectifiers for OBC	■ 50% duty ratio used
		Trapezoidal-Modulation [95]–[99]	-	-	-		■ Involve two duty ratio and PS
		Triangular-Modulation [100]–[102]	20 ~ 50	90	-		■ Special case of TZM
AC-AC	①	Passive Snubber [67]–[70]	12 ~ 100	95	0.2 ~ 3	Inductive heating systems	■ Built by a lossless snubber
		Active Snubber [71]–[74]	5 ~ 150	94	0.5 ~ 0.5	Low-speed AC motor drives	■ Built by an active snubber
	②	Phase-Shift-Modulation [103]–[107]	25 ~ 100	98	0.5 ~ 15	DAB-based AC-AC converters	■ Employ PS between primary and secondary sides
		AC-link [108]–[112]	20 ~ 120	95	0.2 ~ 1.6	Variable speed AC drives	■ Achieved via controlling the frequency of AC-link charging/discharging current

Note that "①" and "②" represent "auxiliary-circuit-based techniques" and "nonauxiliary-circuit-based techniques," respectively.

techniques discussed above, which provides useful information about each technique: switching frequency, efficiency, and power level. In addition, it gives some direction on suitable applications and points out some highlights for every technique.

V. FUTURE RESEARCH ISSUES FOR SOFT-SWITCHING TECHNIQUES

This section discusses possible future research issues for soft-switching techniques in power converters.

A. Advanced Power Switches to Achieve High Switching Frequency and High Efficiency

Soft-switching techniques can overcome switching loss, but conduction loss is still one of their major problems. To solve this problem, advanced power switching devices are highly sought after to boost efficiency as they can guarantee soft transition via their low ON-resistance and fast-acting gate with a high switching frequency [113]–[115]. In recent years, wide-band gap (WBG) technologies, e.g., Gallium Nitride (GaN) and Silicon Carbide (SiC), have shown great promise as WBG semiconductors that can achieve high power and frequency ranges (i.e., GaN: 0.1∼10 kW/100 kHz∼100 GHz and SiC: 10 kW∼10 MW/1 kHz∼1 MHz). Therefore, WBG-based power converters have been widely used in various applications,e.g., high efficiency, high power density, high switching frequency, and better thermal capability. Nevertheless, their loss behavior significantly varies between different WBG technologies, e.g., dynamic ON-state resistance ($R_{DS(ON)}$) degradation, output capacitance (C_{OSS}) charging/discharging time, etc. [116], [117].

TABLE II
COMPARISON OF SOME WBG TECHNOLOGIES

WBT Technology	V_{BR} (V)	I_{DS} (A)	Q_G (nC)	$R_{DS(ON)}$ (m Ω)	C_{OSS} (pF)
GS66508T (P-GaN-Gated)	650	30	5.8	50	65
TP65H050WS (GaN-Cascode)	650	36	16	50	130
SCT3060AL (SiC)	650	39	58	60	85
UF3C065080K3S (SiC Cascode)	650	31	51	80	62

For instance, cascode arrangement reduces gate losses in SiC devices but increases threshold voltage for GaN devices [113]–[117]. Besides, GaN power devices can significantly achieve increased power density in power converters owing to the aforementioned features. Meanwhile, SiC power devices can tolerate more heat than GaN power devices because of their high thermal conductivity. Also, a reverse voltage blocking capability along with a series SiC Schottky diode helps in acheiving ZVS-turn-ON in current source converter applications [118], [119]. Consequently, they can be used in a wide range of industrial applications, e.g., data centers, EVs, smart mobility, smart grid, smart transport, smart manufacturing, etc. to achieve high efficiency while maintaining high switching frequency [113]–[119].

Table II compares some WBG technologies such as GaN and SiC power devices. It can be observed from this table that the breakdown voltage (V_{BR}) and drain-source current (I_{DS}) are roughly the same for both switching devices, but the gate-charge (Q_{G}), ON-resistance ($R_{\mathrm{DS(ON)}}$), and output capacitance (C_{OSS}) of GaN-based switches are slightly bigger than those of SiC-based ones [114]–[117].

B. Simple Topologies for Reduced Power Devices

Next, simple power converter topologies with reduced power devices are highly demanded to achieve higher power densities and simple control [121], [123]. In fact, simple topologies not only simplify the control of power converters, but also improve the power density (volume and mass) of power converters [122], [123]. Further, simple topologies negate the need for massive heat sinks to ensure that the device is cooled appropriately [4], [6], [37]. As such, there are several research challenges to come out of these simplified power converter topologies that use smaller numbers of switching devices to improve the switching action of the power devices that comes from the more reliable power topologies [122]–[124].

C. Advanced Control Schemes Associated With Improved Phase-Shift Techniques

Finally, advanced control schemes associated with improved PSM and current regulation (e.g., PSM, DPS, CC-based techniques [125], [126], triple-phase-shift (TPS) control techniques, [127], [128], etc.) can make soft switching in power converters more effective because they can remarkably extend the soft-switching range for advanced switching devices. For example, the TPS control strategy provides a load matching that can achieve ZVS for the whole power switches during the entire power range [127], [128]. Such techniques hold great interest for both current and future applications (e.g., OBCs, wireless power transfer, integrated motor drives, etc.) because they allow a single power device to function in different modes while achieving higher power density, compact size, improved fault tolerance, etc. [19], [114].

VI. CONCLUSION

This article presented an extensive review on state-of-the-art soft-switching techniques for power converters. Soft-switching techniques had received a great deal of interest from researchers in the field of power converter applications due to the growing requirements for high switching frequencies while retaining high efficiency of the switched-mode power electronic converters on a reduced scale. It comprehensively discussed the soft-switching techniques that ensure ZVS and ZCS in semiconductor switching devices (e.g., MOSFETs, IGBTs, etc.). First, the auxiliary-circuit-based and nonauxiliary-circuit-based techniques to achieve soft switching were systematically categorized according to the type of power converter they are used in. Next, all methods for each converter type were individually discussed in detail. Last, it offered some valuable direction on suitable applications for ZVS and ZCS in accordance with potential future research developments in soft-switching techniques for power converters.

REFERENCES

[1] D. Y. Lee, B. K. Lee, S. B. Yoo, and D. S. Hyun, “An improved full-bridge zero-voltage-transition PWM DC/DC converter with zero-voltage/zero-current switching of the auxiliary switches,” *IEEE Trans. Ind. Appl.*, vol. 36, no. 2, pp. 558–566, Apr. 2000.

[2] T. Bang and J. W. Park, “Development of a ZVT-PWM buck cascaded buck–boost PFC converter of 2 kw with the widest range of input voltage,” *IEEE Trans. Ind. Electron.*, vol. 65, no. 3, pp. 2090–2099, Mar. 2018.

[3] C. M. Wang, “Novel zero-voltage-transition PWM DC-DC converters,” *IEEE Trans. Ind. Electron.*, vol. 53, no. 1, pp. 254–262, Feb. 2006.

[4] J. Lyu, B. Ma, H. Yan, Z. Ji, and J. Ding, “A modified finite control set model predictive control for 3*L*-NPC grid-connected inverters using virtual voltage vectors,” *J. Elect. Eng. Technol.*, vol. 15, no. 6, pp. 121–133, Oct. 2020.

[5] M. H. Rashid, *Power Electronics Handbook: Devices, Circuits, and Applications Handbook*, 4th ed., Oxford, U.K.: Butterworth-Heinemann, 2018.

[6] J. H. Oh, J. H. Lee, J. C. Ryu, H. W. Lee, H. M. Chae, and J. E. Kim, “Operation method for hybrid UPS with energy storage system function,” *J. Elect. Eng. Technol.*, vol. 14, no. 5, pp. 1871–1880, Sep. 2019.

[7] Y. Zhang, X. F. Cheng, and C. Yin, “A soft-switching non-inverting buck–boost converter with efficiency and performance improvement,” *IEEE Trans. Power Electron.*, vol. 34, no. 12, pp. 11526–11530, Dec. 2019.

[8] S. A. Q. Mohammed, M. S. Rafaq, H. H. Choi, and J. W. Jung, “A robust adaptive PI voltage controller to eliminate impact of disturbances and distorted model parameters for 3-phase CVCF inverters,” *IEEE Trans. Ind. Informat.*, vol. 16, no. 4, pp. 2168–2176, Apr. 2020.

[9] A. Nami, F. Zare, A. Ghosh, and F. Blaabjerg, “Multi-output dc–dc converters based on diode-clamped converters configuration: Topology and control strategy,” *IET Power Electron.*, vol. 3, no. 2, pp. 197–208, Mar. 2010.

[10] S. A. Q. Mohammed, A. T. Nguyen, H. H. Choi, and J. W. Jung, “Improved iterative learning control strategy for surface-mounted permanent magnet synchronous motor drives,” *IEEE Trans. Ind. Electron.*, vol. 67, no. 12, pp. 10134–10144, Dec. 2020.

[11] R. Huang and S. K. Mazumder, "A soft-switching scheme for an isolated DC/DC converter with pulsating DC output for a three-phase high-frequency-link PWM converter," *IEEE Trans. Power Electron.*, vol. 24, no. 10, pp. 2276–2288, Oct. 2009.

[12] S. Jalbrzykowski, A. Bogdan, and T. Citko, "A dual full-bridge resonant class-e bidirectional DC–DC converter," *IEEE Trans. Ind. Electron.*, vol. 58, no. 9, pp. 3879–3883, Sep. 2011.

[13] J. G. Cho and G. H. Cho, "Cyclic quasi-resonant converters: A new group of resonant converters suitable for high performance DC/DC and AC/AC conversion applications," in *Proc. 16th Annu. Conf. IEEE Ind. Electron. Soc.*, 1990, pp. 956–963.

[14] M. Hissem, A. Cheriti, P. Sicard, and A. B. Razzouk, "Application of the current-injected modeling approach to quasi-resonant converters," *IEEE Trans. Power Electron.*, vol. 12, no. 4, pp. 695–703, Jul. 1997.

[15] E. Jayashree and G. Uma, "Analysis, design and implementation of a quasi-resonant DC–DC converter," *IET Power Elect.*, vol. 4, no. 7, pp. 785–792, Dec. 2011.

[16] T. Zhu, F. Zhuo, F. Zhao, F. Wang, H. Yi, and T. Zhao, "Optimization of extended phase-shift control for full-bridge CLLC resonant converter with improved light-load efficiency," *IEEE Trans. Power Electron.*, vol. 35, no. 10, pp. 11129–11142, Oct. 2020.

[17] S. Neira, J. Pereda, and F. Rojas, "Three-port full-bridge bidirectional converter for hybrid DC/DC/AC systems," *IEEE Trans. Power Electron.*, vol. 35, no. 12, pp. 13077–13084, Dec. 2020.

[18] J. Zeng, Z. Yu, J. Liu, and F. Liu, "Triple-compound-full-bridge-based ut converter with wide zero-voltage switching range and wide conversion gain," *IEEE Trans. Ind. Electron.*, vol. 67, no. 11, pp. 9260–9272, Nov. 2020.

[19] L. Costa, G. Buticchi, and M. Liserre, "A fault-tolerant series-resonant DC–DC converter," *IEEE Trans. Power Electron.*, vol. 32, no. 2, pp. 900–905, Feb. 2017.

[20] Y. Du, S. M. Lukic, B. S. Jacobson, and A. Q. Huang, "Modulation technique to reverse power flow for the isolated series resonant DC–DC converter with clamped capacitor voltage," *IEEE Trans. Ind. Electron.*, vol. 59, no. 12, pp. 4617–4628, Dec. 2012.

[21] N. C. D. Pont, D. G. Bandeira, T. B. Lazzarin, and I. Barbi, "A ZVS APWM half-bridge parallel resonant DC–DC converter with capacitive output," *IEEE Trans. Ind. Electron.*, vol. 66, no. 7, pp. 5231–5241, Jul. 2019.

[22] M. Uno, K. Yoshino, and K. Hasegawa, "Direct cell-to-cell voltage equalizer using capacitively-isolated parallel-resonant converter for series-connected energy storage cells," in *Proc. IEEE 18th Int. Power Electron. Motion Control Conf.*, 2018, pp. 94–100.

[23] A. H. M. Dobi, M. R. Sahid, and T. Sutikno, "Overview of soft-switching DC-DC converters," *Int. J. Power Electron. Drive Syst.*, vol. 9, no. 4, pp. 2006–2018, Dec. 2018.

[24] U. Patil and H. Nagendrappa, "Analysis and design of a high frequency isolated full bridge CLL resonant DC-DC converter for renewable energy applications," in *Proc. Int. Conf. Power, Instrum., Control Comput.*, 2018, pp. 1–6.

[25] F. Han, Y. Wang, L. Yang, M. Chen, R. Liu, and R. Xu, "High-efficiency topology-morphing multi-resonant DC–DC converter with wide voltage gain range for small-scale wind generation applications," *IET Power Electron.*, vol. 12, no. 9, pp. 2330–2337, Aug. 2019.

[26] Y. Wang, F. Han, L. Yang, C. Wang, and B. Zhou, "Dual-transformer soft-switching DC–DC resonant converter with multiple resonant elements," *IET Power Electron.*, vol. 11, no. 15, pp. 2538–2544, Dec. 2018.

[27] H. Wu, X. Jin, H. Hu, and Y. Xing, "Multielement resonant converters with a notch filter on secondary side," *IEEE Trans. Power Electron.*, vol. 31, no. 6, pp. 3999–4004, Jun. 2016.

[28] T. Qian, K. Guo, and C. Qian, "A combined three-port LLC structure for adaptive power flow adjustment of PV systems," *IEEE Trans. Power Electron.*, vol. 35, no. 10, pp. 10413–10422, Oct. 2020.

[29] S. Moury and J. Lam, "A soft-switched power module with integrated battery interface for photovoltaic-battery power architecture," *IEEE J. Emerg. Sel. Top. Power Electron.*, vol. 8, no. 3, pp. 3090–3110, Sep. 2020.

[30] F. Musavi, M. Craciun, D. S. Gautam, W. Eberle, and W. G. Dunford, "An LLC resonant DC–DC converter for wide output voltage range battery charging applications," *IEEE Trans. Power Electron.*, vol. 28, no. 12, pp. 5437–5445, Dec. 2013.

[31] F. Han, Y. Wang, L. Yang, C. Wang, R. Liu, and Z. Meng, "Family of DTMRC-based DC–DC converters with an RZP," *IET Power Electron.*, vol. 13, no. 3, pp. 505–515, Feb. 2020.

[32] S. Urgun, "Zero-voltage transition–zero-current transition pulsewidth modulation DC–DC buck converter with zero-voltage switching–zero-current switching auxiliary circuit," *IET Power Electron.*, vol. 5, no. 5, pp. 627–634, May 2012.

[33] S. Dusmez, A. Khaligh, and A. Hasanzadeh, "A zero-voltage-transition bidirectional DC/DC converter," *IEEE Trans. Ind. Electron.*, vol. 62, no. 5, pp. 3152–3162, May 2015.

[34] Y. P. B. Yeung and K. W. E. Cheng, "Zero-current switching fixed frequency resonant-transition square wave converters," *IEEE Proc. Elect. Power Appl.*, vol. 148, no. 6, pp. 475–480, Nov. 2001.

[35] U. Patil and N. Harischandrappa, "Analysis and design of a high-frequency isolated full-bridge ZVT CLL resonant DC–DC converter," *IEEE Trans. Ind. Appl.*, vol. 55, no. 5, pp. 4993–5004, Sep. 2019.

[36] D. Y. Lee, M. K. Lee, D. K. Hyun, and I. Choy, "New zero-current-transition PWM DC/DC converters without current stress," *IEEE Trans. Power Electron.*, vol. 18, no. 1, pp. 95–104, Jan. 2003.

[37] M. M. Walters and W. M. Polivka, "Extending the range of soft-switching in resonant-transition DC-DC converters," in *Proc. 14th Int. Telecommun. Energy Conf.*, 1992, pp. 343–350.

[38] C. T. Rim and G. H. Cho, "Phasor transformation and its application to the DC/AC analyses of frequency phase-controlled series resonant converters (SRC)," *IEEE Trans. Power Electron.*, vol. 5, no. 2, pp. 201–211, Apr. 1990.

[39] P. K. Jain, J. R. Espinoza, and S. B. Dewan, "Self-started voltage-source series-resonant converter for high-power induction heating and melting applications," *IEEE Trans. Ind. Appl.*, vol. 34, no. 3, pp. 518–525, Jun. 1998.

[40] C. S. Moo, Y. C. Chuang, and J. C. Lee, "A new dynamic filter for the electronic ballast with the parallel-load resonant inverter," in *Proc. IEEE Ind. Appl. Conf. 30th IAS Annu. Meeting*, 1995, pp. 2597–2601.

[41] A. Damrong, P. Suttichai, and K. Higuchi, "An improved soft-switching single-phase inverter for small grid-connected PV-system," in *Proc. 34th Annu. Conf. IEEE Ind. Electron.*, 2008, pp. 2125–2130.

[42] S. C. Wong and A. D. Brown, "Parallel resonant converter as a circuit simulation primitive," *IEE Proc. Circuits Devices Syst.*, vol. 142, no. 6, pp. 379–386, Dec. 1995.

[43] P. Vishnuram, G. Ramachandiran, S. Ramasamy, and S. Dayalan, "A comprehensive overview of power converter topologies for induction heating applications," *Int. Trans. Elect. Energy Syst.*, vol. 30, no. 10, pp. 1–33, Oct. 2020.

[44] G. W. Koo, W. Y. Sung, and B. K. Lee, "Comparison and design of resonant network considering the characteristics of a plasma generator," *Energies*, vol. 12, no. 16, Aug. 2019, Art. no. 3156.

[45] T. Nakamizo, M. Kaneda, S. Hishikawa, B. Guo, H. Iwamoto, and M. Nakaoka, "New generation fluid heating appliance using high-frequency load resonant inverter," in *Proc. IEEE Int. Conf. Power Electron. Drive Syst.*, 1999, pp. 309–314.

[46] Z. Ye, P. K. Jain, and P. C. Sen, "A two-stage resonant inverter with control of the phase angle and magnitude of the output voltage," *IEEE Trans. Ind. Electron.*, vol. 57, no. 5, pp. 2797–2812, Oct. 2007.

[47] Y. Li and F. C. Lee, "A generalized zero-current-transition concept to simplify multilevel ZCT converters," *IEEE Trans. Ind. Appl.*, vol. 42, no. 5, pp. 1310–1320, Sep. 2006.

[48] Y. P. Li, F. C. Lee, and D. Boroyevich, "A simplified three-phase zero-current-transition inverter with three auxiliary switches," *IEEE Trans. Power Electron.*, vol. 18, no. 3, pp. 802–813, May 2003.

[49] Y. Li, F. C. Lee, and D. Boroyevich, "A three-phase soft-transition inverter with a novel control strategy for zero-current and near zero-voltage switching," *IEEE Trans. Power Electron.*, vol. 16, no. 5, pp. 710–723, Sep. 2001.

[50] Y. P. Li, F. C. Lee, and D. Boroyevich, "IGBT device application aspects for 50-kW zero-current-transition inverters," *IEEE Trans. Ind. Appl.*, vol. 40, no. 4, pp. 1039–1048, Jul. 2004.

[51] V. V. Deshpande and S. Rao Doradla, "A detailed study of loss in the reduced voltage resonant link inverter topology," *IEEE Trans. Power Electron.*, vol. 13, no. 2, pp. 337–344, Mar. 1998.

[52] Y. P. Li, F. C. Lee, and D. Boroyevich, "A simplified three-phase zero-current-transition inverter with three auxiliary switches," *IEEE Trans. Power Electron.*, vol. 18, no. 3, pp. 802–813, May 2003.

[53] Y. C. Jung, H. L. Liu, G. C. Cho, and G. H. Cho, "Soft switching space vector PWM inverter using a new quasi-parallel resonant DC link," in *Proc. Power Electron. Specialist Conf.*, 1995, pp. 936–942.

[54] F. M. Ibanez, "Bidirectional series resonant DC/AC converter for energy storage systems," *IEEE Trans. Power Electron.*, vol. 34, no. 4, pp. 3429–3444, Apr. 2019.

[55] T. Bruckner and S. Bernet, "Investigation of a high-power three-level quasi-resonant DC-link voltage-source inverter," *IEEE Trans. Ind. Appl.*, vol. 37, no. 2, pp. 619–627, Apr. 2001.

[56] M. Ishida, H. Fujino, and T. Hori, "Real-time output voltage control method of quasi-ZCS series resonant HF-linked DC-AC converter," *IEEE Trans. Power Electron.*, vol. 10, no. 6, pp. 776–783, Nov. 1995.

[57] M. Amirabadi, J. Baek, and H. A. Toliyat, "Ultrasparse AC-Link converters," *IEEE Trans. Ind. Appl.*, vol. 51, no. 1, pp. 448–458, Jan. 2015.

[58] D. Rothmund, D. Bortis, J. Huber, D. Biadene, and J. W. Kolar, "10kV SiC-based bidirectional soft-switching single-phase AC/DC converter concept for medium-voltage solid-state transformers," in *Proc. IEEE 8th Int. Symp. Power Electron. Distrib. Gener. Syst.*, 2017, pp. 1–8.

[59] H. Pinheiro, P. Jain, and G. Joos, "Self-oscillating resonant AC/DC converter topology for input power-factor correction," *IEEE Trans. Ind. Electron.*, vol. 46, no. 4, pp. 692–702, Aug. 1999.

[60] M. Narimani and G. Moschopoulos, "A new single-phase single-stage three-level power-factor-correction AC–DC converter with phase-shift modulation," *IEEE Trans. Ind. Electron.*, vol. 60, no. 9, pp. 3731–3735, Sep. 2013.

[61] C. M. Wang, "A novel soft-switching single-phase DC-AC converter using new ZVS PWM strategy," *IEEE Trans. Power Electron.*, vol. 22, no. 5, pp. 1941–1948, Sep. 2007.

[62] H. Valipour, M. Mahdavi, and M. Ordonez, "Resonant bridgeless AC/DC rectifier with high switching frequency and inherent PFC capability," *IEEE Trans. Power Electron.*, vol. 35, no. 1, pp. 232–246, Jan. 2020.

[63] H. Belkamel, H. Kim, and S. Choi, "Interleaved totem-pole ZVS converter operating in CCM for single-stage bidirectional AC–DC conversion with high-frequency isolation," *IEEE Trans. Power Electron.*, vol. 36, no. 3, pp. 3486–3495, Mar. 2021.

[64] M. Alam, W. Eberle, D. S. Gautam, and C. Botting, "A soft-switching bridgeless AC-DC power factor correction converter," *IEEE Trans. Power Electron.*, vol. 32, no. 10, pp. 7716–7726, Oct. 2017.

[65] M. Pahlevaninezhad, P. Das, J. Drobnik, P. K. Jain, and A. Bakhshai, "A ZVS interleaved boost AC/DC converter used in plug-in electric vehicles," *IEEE Trans. Power Electron.*, vol. 27, no. 8, pp. 3513–3529, Aug. 2012.

[66] S. H. Lee, W. J. Cha, and B. H. Kwon, "High-efficiency soft-switching AC–DC converter with single-power-conversion method," *IEEE Trans. Ind. Electron.*, vol. 64, no. 6, pp. 4483–4490, Jun. 2017.

[67] T. Mishima, Y. Nakagawa, and M. Nakaoka, "A bridgeless BHB ZVS-PWM AC–AC converter for high-frequency induction heating applications," *IEEE Trans. Ind. Appl.*, vol. 51, no. 4, pp. 3304–3315, Jul. 2015.

[68] S. Samanta and A. K. Rathore, "A new inductive power transfer topology using direct AC–AC converter with active source current waveshaping," *IEEE Trans. Power Electron.*, vol. 33, no. 7, pp. 5565–5577, Jul. 2018.

[69] H. Keyhani and H. A. Toliyat, "Isolated ZVS high-frequency-link AC-AC converter with a reduced switch count," *IEEE Trans. Power Electron.*, vol. 29, no. 8, pp. 4156–4166, Aug. 2014.

[70] W. Guo and P. K. Jain, "A low frequency AC to high frequency AC inverter with build-in power factor correction and soft-switching," *IEEE Trans. Power Electron.*, vol. 19, no. 2, pp. 430–442, Mar. 2004.

[71] R. Teichmann and J. Oyama, "ARCP soft-switching technique in matrix converters," *IEEE Trans. Ind. Electron.*, vol. 49, no. 2, pp. 353–361, Apr. 2002.

[72] A. Safaee, D. Yazdani, A. Bakhshai, and P. K. Jain, "Multiblock soft-switched bidirectional AC–AC converter using a single loss-less active snubber block," *IEEE Trans. Power Electron.*, vol. 27, no. 5, pp. 2260–2272, May 2012.

[73] A. Iyer, R. Moghe, R. Kandula, A. Prasai, and D. Divan, "Experimental validation of active snubber circuit for direct AC/AC converters," in *Proc. IEEE Energy Convers. Congr. Expo.*, 2012, pp. 3856–3861.

[74] A. Prasai and D. Divan, "Active AC snubber for direct AC/AC power converters," in *Proc. IEEE Energy Convers. Congr. Expo.*, 2011, pp. 507–514.

[75] I. Kayaalp, T. Demirdelen, T. Koroglu, M. U. Cuma, K. C. Bayindir, and M. Tumay, "Comparison of different phase-shift control methods at isolated bidirectional DC-DC converter," *Int. J. Appl. Math. Electron. Comput.*, vol. 4, no. 3, pp. 68–73, Aug. 2016.

[76] X. Fei, Z. Feng, N. Puqi, and W. Xuhui, "Analyzing ZVS soft switching using single phase shift control strategy of dual active bridge isolated DC-DC converters," in *Proc. 21st Int. Conf. Elect. Mach. Syst.*, 2018, pp. 2378–2381.

[77] A. Kumar, A. H. Bhat, and P. Agarwal, "Comparative analysis of dual active bridge isolated DC to DC converter with single phase shift and extended phase shift control techniques," in *Proc. 6th Int. Conf. Comput. Appl. Elect. Eng.-Recent Adv.*, 2017, pp. 397–402.

[78] K. E. Lucas, D. J. Pagano, and R. L. P. Medeiros, "Single phase-shift control of DAB converter using robust parametric approach," in *Proc. IEEE 15th Braz. Power Electron. Conf. 5th IEEE Southern Power Electron. Conf.*, 2019, pp. 1–6.

[79] M. Hong, G. Xuanjie, Z. Chengbi, and D. Shujiang, "An improved dual phase shift control strategy for dual active bridge DC-DC converter with soft switching," in *Proc. Int. Power Electron. Conf.*, 2018, pp. 2718–2724.

[80] S. Tiwari and S. Sarangi, "Implementation of SPS and DPS control techniques on DAB converter with comparative analysis," *J. Inf. Optim. Sci.*, vol. 40, no. 8, pp. 1623–1638, Nov. 2019.

[81] Z. Zhang, S. Xie, Z. Wu, and J. Xu, "Soft-switching and low conduction loss current-fed isolated bidirectional DC–DC converter with PWM plus dual phase-shift control," *J. Power Electron.*, vol. 20, no. 3, pp. 664–674, May 2020.

[82] M. Kim, M. Rosekeit, S. K. Sul, and R. W. A. A. De Doncker, "A dual-phase-shift control strategy for dual-active-bridge DC-DC converter in wide voltage range," in *Proc. 8th Int. Conf. Power Electron.*, May 2011, pp. 364–371.

[83] N. Hou and Y. W. Li, "Overview and comparison of modulation and control strategies for a nonresonant single-phase dual-active-bridge DC–DC converter," *IEEE Trans. Power Electron.*, vol. 35, no. 3, pp. 3148–3172, Mar. 2020.

[84] A. Amirahmadi *et al.*, "Hybrid ZVS BCM current controlled three-phase microinverter," *IEEE Trans. Power Electron.*, vol. 29, no. 4, pp. 2124–2134, Apr. 2014.

[85] D. Sha, J. Zhang, and J. Wu, "A gan-based microconverter utilizing fixed-frequency BCM control method for PV applications," *IEEE Trans. Ind. Electron.*, vol. 65, no. 6, pp. 4771–4780, Jun. 2018.

[86] Q. Zhang, H. Hu, D. Zhang, X. Fang, Z. J. Shen, and I. Bartarseh, "A controlled-type ZVS technique without auxiliary components for the low power DC/AC inverter," *IEEE Trans. Power Electron.*, vol. 28, no. 7, pp. 3287–3296, Jul. 2013.

[87] A. Amirahmadi, L. Chen, U. Somani, H. Hu, N. Kutkut, and I. Bartarseh, "High efficiency dual-mode current modulation method for low-power DC/AC inverters," *IEEE Trans. Power Electron.*, vol. 29, no. 6, pp. 2638–2642, Jun. 2014.

[88] C. M. Wang, "Nonlinear-controlled strategy for soft-switched series-resonant DC/AC inverter without auxiliary switches," *IEEE Trans. Power Electron.*, vol. 18, no. 3, pp. 764–774, May 2003.

[89] D. Serrano, R. Ramos, P. Alou, J. A. Oliver, and J. A. Cobos, "Multimode modulation with ZVS for a single-phase single-stage inverter," *IEEE Trans. Power Electron.*, vol. 35, no. 5, pp. 5319–5330, May 2020.

[90] M. Llomplat, J. E. Bosso, R. E. Carballo, and G. O. Garcia, "Novel modified phase-shift modulation strategy for isolated AC–DC power converters," *IET Power Electron.*, vol. 13, no. 5, pp. 1022–1032, Apr. 2020.

[91] O. C. D. S. Filho, B. R. de Almeida, D. D. S. O. Junior, and T. R. F. Neto, "High-frequency isolated AC–DC–AC interleaved converter for power quality applications," *IEEE Trans. Ind. Appl.*, vol. 54, no. 5, pp. 4594–4602, Sep./Oct. 2018.

[92] S. Zengin and M. Boztepe, "A novel current modulation method to eliminate low-frequency harmonics in single-stage dual active bridge AC–DC converter," *IEEE Trans. Ind. Electron.*, vol. 67, no. 2, pp. 1048–1058, Feb. 2020.

[93] H. Zhou and A. M. Khambadkone, "Hybrid modulation for dual-active-bridge bidirectional converter with extended power range for ultracapacitor application," *IEEE Trans. Ind. Appl.*, vol. 45, no. 4, pp. 1434–1442, Jul. 2009.

[94] F. Krismer, S. Round, and J. W. Kolar, "Performance optimization of a high current dual active bridge with a wide operating voltage range," in *Proc. 37th IEEE Power Electron. Specialists Conf.*, 2006, pp. 1–7.

[95] S. Norrga, S. Meier, and S. Ostlund, "A three-phase soft-switched isolated AC/DC converter without auxiliary circuit," *IEEE Trans. Ind. Appl.*, vol. 44, no. 3, pp. 836–844, May/Jun. 2008.

[96] S. Norrga, "Experimental study of a soft-switched isolated bidirectional AC-DC converter without auxiliary circuit," *IEEE Trans. Power Electron.*, vol. 21, no. 6, pp. 1580–1587, Nov. 2006.

[97] J. Everts, F. Krismer, J. Van den Keybus, J. Driesen, and J. W. Kolar, "Charge-based ZVS soft switching analysis of a single-stage dual active bridge AC-DC converter," in *Proc. IEEE Energy Convers. Congr. Expo.*, 2013, pp. 4820–4829.

[98] J. Everts, F. Krismer, J. Van den Keybus, J. Driesen, and J. W. Kolar, "Comparative evaluation of soft-switching, bidirectional, isolated AC/DC converter topologies," in *Proc. 27th Annu. IEEE Appl. Power Electron. Conf. Expo.*, 2012, pp. 1067–1074.

[99] A. Abasian, H. F. fard, and S. Madani, "Single stage soft switching AC/DC converter without any extra switch," *IET Power Electron.*, vol. 7, no. 3, pp. 745–752, Mar. 2014.
[100] J. Everts, F. Krismer, J. Van den Keybus, J. Driesen, and J. W. Kolar, "Optimal ZVS modulation of single-phase single-stage bidirectional DAB AC–DC converters," *IEEE Trans. Power Electron.*, vol. 29, no. 8, pp. 3954–3970, Aug. 2014.
[101] G. Castelino, K. Basu, N. Weise, and N. Mohan, "A bi-directional, isolated, single-stage, DAB-based AC-DC converter with open-loop power factor correction and other advanced features," in *Proc. IEEE Int. Conf. Ind. Technol.*, 2012, pp. 938–943.
[102] J. Everts, J. Van den Keybus, F. Krismer, J. Driesen, and J. W. Kolar, "Switching control strategy for full ZVS soft-switching operation of a dual active bridge AC/DC converter," in *Proc. 27th Annu. IEEE Appl. Power Electron. Conf. Expo.*, 2012, pp. 1048–1055.
[103] W. Guo and P. K. Jain, "A low frequency AC to high frequency AC inverter with build-in power factor correction and soft-switching," *IEEE Trans. Power Electron.*, vol. 19, no. 2, pp. 430–442, Mar. 2004.
[104] S. K. Mazumder and A. K. Rathore, "Primary-side-converter-assisted soft-switching scheme for an AC/AC converter in a cycloconverter-type high-frequency-link inverter," *IEEE Trans. Ind. Electron.*, vol. 58, no. 9, pp. 4161–4166, Sep. 2011.
[105] T. Mishima, S. Sakamoto, and C. Ide, "ZVS phase-shift PWM-controlled single-stage boost full-bridge AC–AC converter for high-frequency induction heating applications," *IEEE Trans. Ind. Electron.*, vol. 64, no. 3, pp. 2054–2061, Mar. 2017.
[106] H. Qin and J. W. Kimball, "Solid-state transformer architecture using AC-AC dual-active-bridge converter," *IEEE Trans. Ind. Electron.*, vol. 60, no. 9, pp. 3720–3730, Sep. 2013.
[107] O. Korkh, A. Blinov, and D. Vinnikov, "Analysis of oscillation suppression methods in the AC-AC stage of high frequency link converters," in *Proc. IEEE 60th Int. Sci. Conf. Power Elect. Eng. Riga Tech. Univ.*, 2019, pp. 1–5.
[108] M. Amirabadi, J. Baek, H. A. Toliyat, and W. C. Alexander, "Soft-switching AC-link three-phase AC–AC buck–boost converter," *IEEE Trans. Ind. Electron.*, vol. 62, no. 1, pp. 3–14, Jan. 2015.
[109] S. A. Kh. M. Niapour and M. Amirabadi, "Extremely sparse parallel AC-Link universal power converters," *IEEE Trans. Ind. Appl.*, vol. 52, no. 3, pp. 2456–2466, May 2016.
[110] E. Afshari, M. Khodabandeh, and M. Amirabadi, "A single-stage capacitive AC-link AC–AC power converter," *IEEE Trans. Power Electron.*, vol. 34, no. 3, pp. 2104–2118, Mar. 2019.
[111] K. Mozaffari and M. Amirabadi, "A highly reliable and efficient class of single-stage high-frequency AC-link converters," *IEEE Trans. Power Electron.*, vol. 34, no. 9, pp. 8435–8452, Sep. 2019.
[112] H. Akagi, "The state-of-the-art of power electronics in Japan," *IEEE Trans. Power Electron.*, vol. 13, no. 2, pp. 345–356, Mar. 1998.
[113] M. H. Ahmed, C. Fei, F. C. Lee, and Q. Li, "Single-stage high-efficiency 48/1 v sigma converter with integrated magnetics," *IEEE Trans. Ind. Electron.*, vol. 67, no. 1, pp. 192–202, Jan. 2020.
[114] A. Jafari *et al.*, "Comparison of wide-band-gap technologies for soft-switching losses at high frequencies," *IEEE Trans. Power Electron.*, vol. 35, no. 12, pp. 12595–12600, Dec. 2020.
[115] M. Shur, "Wide band gap semiconductor technology: State-of-the-art," *Solid-State Electron.*, vol. 155, pp. 65–75, May 2019.
[116] F. Roccaforte *et al.*, "Emerging trends in wide band gap semiconductors (SiC and GaN) technology for power devices," *Microelectron. Eng.*, vol. 187/188, pp. 66–77, Feb. 2018.
[117] A. Agarwal *et al.*, "Wide band gap semiconductor technology for energy efficiency," *Mater. Sci. Forum*, vol. 858, pp. 797–802, May 2016.
[118] B. Akhlaghi and H. Farzanehfard, "Family of ZVT interleaved converters with low number of components," *IEEE Trans. Ind. Electron.*, vol. 65, no. 11, pp. 8565–8573, Nov. 2018.
[119] S. Hazra *et al.*, "High switching performance of 1700-V, 50-A SiC power MOSFET over si IGBT/BiMOSFET for advanced power conversion applications," *IEEE Trans. Power Electron.*, vol. 31, no. 7, pp. 4742–4754, Jul. 2016.
[120] S. Khan, D. Sha, X. Jia, and S. Wang, "Resonant LLC DC–DC converter employing fixed switching frequency based on dual-transformer with wide input-voltage range," *IEEE Trans. Power Electron.*, vol. 36, no. 1, pp. 607–616, Jan. 2021.
[121] B. M. Tehrani, M. A. Chamali, E. Adib, M. R. Amini, and D. G. Najafabadi, "Introducing self-oscillating technique for a soft-switched LED driver," *IEEE Trans. Ind. Electron.*, vol. 65, no. 8, pp. 6160–6167, Aug. 2018.
[122] D. O. Bamgboje, W. Harmon, M. Tahan, and T. Hu, "Low cost high performance LED driver based on a self-oscillating boost converter," *IEEE Trans. Power Electron.*, vol. 34, no. 10, pp. 10021–10034, Oct. 2019.
[123] M. Khodabandeh, E. Afshari, and M. Amirabadi, "A single-stage soft-switching high-frequency AC-link PV inverter: Design, analysis, and evaluation of Si-based and sic-based prototypes," *IEEE Trans. Power Electron.*, vol. 34, no. 3, pp. 2312–2326, Mar. 2019.
[124] H. Keyhani and H. A. Toliyat, "A soft-switched three-phase AC–AC converter with a high-frequency AC link," *IEEE Trans. Ind. Appl.*, vol. 50, no. 4, pp. 2637–2647, Jul. 2014.
[125] X. Zhou, J. Xu, and S. Zhong, "Single-stage soft-switching low-distortion bipolar PWM modulation high-frequency-link DC–AC converter with clamping circuits," *IEEE Trans. Ind. Electron.*, vol. 65, no. 10, pp. 7719–7729, Oct. 2018.
[126] A. Jafari, M. S. Nikoo, F. Karakaya, and E. Matioli, "Enhanced DAB for efficiency preservation using adjustable-tap high-frequency transformer," *IEEE Trans. Power Electron.*, vol. 35, no. 7, pp. 6673–6677, Jul. 2020.
[127] X. Zhang *et al.*, "A control strategy for efficiency optimization and wide ZVS operation range in bidirectional inductive power transfer system," *IEEE Trans. Ind. Electron.*, vol. 66, no. 8, pp. 5958–5969, Aug. 2019.
[128] D. Sha, X. Wang, and D. Chen, "High-efficiency current-fed dual active bridge DC–DC converter with ZVS achievement throughout full range of load using optimized switching patterns," *IEEE Trans. Power Electron.*, vol. 33, no. 2, pp. 1347–1357, Feb. 2018.

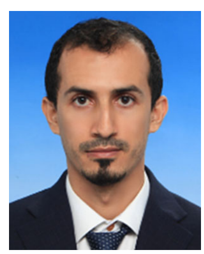

Sadeq Ali Qasem Mohammed received the B.S. degree in electrical engineering from University Tun Hussein Onn Malaysia, Johor, Malaysia, in 2012, and the M.S. degree from the Division of Electrical and Information Engineering from Seoul National University of Science and Technology, Seoul, South Korea, in 2016. He is currently working toward the Ph.D. degree with the Division of Electronics and Electrical Engineering, Dongguk University, Seoul, South Korea.

From 2012 to 2013, he was a Research Assistant with the University Tun Hussein Onn Malaysia. His research interests include distributed generation systems, electric vehicles, and DSP-based electric machine drives.

Jin-Woo Jung (Member, IEEE) received the B.S. and M.S. degrees in electrical engineering from Hanyang University, Seoul, South Korea, in 1991 and 1997, respectively, and the Ph.D. degree in electrical and computer engineering from The Ohio State University, Columbus, OH, USA, in 2005.

From 1997 to 2000, he was with the Home Appliance Research Laboratory, LG Electronics Company, Ltd., Seoul. From 2005 to 2008, he was a Senior Engineer with the R&D Center and with the PDP Development Team, Samsung SDI Company, Ltd., Seoul. Since 2008, he has been a Professor with the Division of Electronics and Electrical Engineering, Dongguk University, Seoul. His research interests include DSP-based electric machine drives, distributed generation systems using renewable energy sources, and power conversion systems and drives for electric vehicles.